ISSN 1990-7931, Russian Journal of Physical Chemistry B, 2025, Vol. 19, No. 2, pp. 388–400. © Pleiades Publishing, Ltd., 2025.

ELECTRIC AND MAGNETIC PROPERTIES OF CHEMICAL COMPOUNDS

Solid-State Lithium-Ion Batteries Based on Using Ionics Conductivity Polymers Interfaces during Interaction between Solid Electrolytes with Both Electrodes

M. Monajjemi[a], *, F. Mollaamin[b], M. Dehghandar[c], R. Tohidloo[c], G. Arab[a], and S. Shahriari[d]

[a] *Department of Chemical Engineering, Central Tehran Branch, Islamic Azad University, Tehran, Iran*

[b] *Department of Biomedical Engineering, Faculty of Engineering and Architecture, Kastamonu University, Kastamonu, Turkey*

[c] *Department of Chemical Engineering, Science and Research branch, Islamic Azad University, Tehran, Iran*

[d] *Department of Chemistry, Central Tehran Branch, Islamic Azad University, Tehran, Iran*

** e-mail: maj.monajjemi@iauctb.ac.ir, m_monajjemi@yahoo.com*

Received April 1, 2024; revised October 16, 2024; accepted October 21, 2024

Abstract—All-solid-state batteries (ASSBs) have come into focus in recent years as energy storage devices with energy densities potentially exceeding those of conventional lithium-ion batteries (LIBs). However, in practice, severe problems still must be solved. To reach high energy densities, it is indispensable to use lithium as anode and to build composite cathodes with high active material loading in the range of 85 wt %. In order to achieve fast ion transport inside the cathode despite the high active material loading, the solid electrolyte should have a high ionic conductivity and should form a continuous phase with low tortuosity ion transport pathways. By this research, we tested the conductivity amounts from various substrates containing amorphous glass, SSBM, and with glass-ceramic samples. Via SSBM technique, silicon nanoparticles were used as anode material, and it was exhibited the charge and discharge curves in the battery cell was cycled between 0.01 and 1.5 V versus Li^+/Li at a current density of 220 mA g^{-1} at room temperature. Since the high resistance, causes degradation of the interface between the cathode material ($LiCoO_2$) and the solid electrolyte, we added GeS_2 and SiS_2 to the $Li_2S-P_2S_5$ system for obtaining higher conductivities and better stability of the electrode/electrolyte interface.

Keywords: solid electrolytes, lithium-ion batteries, ionic conductivity, cathode materials, lithium phosphorus oxy-nitride (LIPON), single step ball milling (SSBM), lithium super-ionic conductor (SILICON), Xrd, charge/discharge curves

DOI: 10.1134/S1990793125700113

1. INTRODUCTION

The influence of interfaces represents a critical factor affecting the use of solid-state batteries (SSBs) in a wide range of practical industrial applications. However, our current understanding of this key issue remains somewhat limited. Therefore, this work presents the mechanisms and advanced characterization techniques associated with interfaces in SSBs. By this study we discuss different aspects of interfaces including interphase formation, cathode-electrolyte interface, anode-electrolyte interface, and inter particle interface, which contain a detailed description of the formation mechanisms and current research. In addition, we summarize the scientific issues associated with solid-solid interfaces and provide our perspectives to better understand the fundamental issues and improve the performance of SSBs. Obviously, safety problem and limited energies densities are the main issues of current LIBs that feature organic liquid electrolytes. In contrast, the development of Li-air/Li anodes [1–4], Li-S anodes [5–8] and Si anodes [9, 10] exhibit promise for increasing energy density, providing that certain challenges can be overcome. For example, sharp, sticky Li dendrites that grow on the Li-metal anode during cycling, which can then penetrate through the separator between two electrodes, will induce sudden failure of the battery and the unwanted release of heat, the result of which is an increased fire hazard due to short-circuiting. For a Li-S battery, in addition to safety concerns associated with dendrites, the polysulfide that form during cycling can dissolve into the liquid electrolytes, thus rendering the cell life too short for most applications without specified electrode modifications [11–14]. During the initial development of viable SSEs, it was evident that the main challenges would be preparing a solid-state material with sufficiently high lithium-ion conductivity, sufficiently high electrical resistivity, favorable temperature stability and good stability in contact with typical LIB electrodes. The information

Table 1. A total comparison of liquid lithium-ion batteries with solid-state model

Liquid cell	Solid-state cell
Inexpensive processing	Expensive processing
Large format in production	Only small format in production
Flexible separator accommodates some mechanical stress	Ceramic separator. Rigid, may break with mechanical stress
Low interfacial impedance	Interfacial impedance can be a problem
Higher ionic conductivity near room temperature	High ionic conductivity over broader temperature range
High electrical resistance	High electrical resistance
Electrolyte flammable, combustion hazard	Electrolyte nonflammable, safer
SEI layer forms and degrades, affects cycle life	No SEI layer formation, longer cycle life
Electrolyte reactions limit cathode materials	Electrolyte nonvolatile, high-voltage cathode materials
Poor thermal stability	Excellent thermal stability
Self-discharge limits shelf life	Far less self-discharge, much longer shelf life
Sensitive to overcharge	Abuse tolerant
Flexible separator hosts formation of lithium dendrites, limits cycle life	Ceramic separator inhibits dendrite growth, extended cycle life
More inactive materials, reduces energy density, reduces specific energy	Less inactive materials increase energy density, increases specific energy

in Table 1 and Fig. 1 exhibits a schematic comparison of liquid electrolyte LIBs and thin-film SSE batteries. Early work [15] revealed LiN_3 to have ionic conductivity comparable with liquid electrolytes, but the electrical resistivity was too low to prove viable as an effective SSE. Researchers also investigated several lithium-ion-conducting compounds, including lithium phosphor silicate glasses, [16] and glass–ceramic compounds [17].

Although in advanced technologies, liquid electrolytes are the most electrolyte application for LIBs fabrication, usage of these type electrolytes are so hazardous and flammable within batteries. Therefore due to a suitable fabricate LIBs with extreme degree of safety; the liquid electrolytes should be changed with solid electrolytes. Solid electrolyte has several advantages compared with liquid electrolytes including large stability, long life containing durable properties, nonflammable, and insulate for preventing thermal increasing inside internal circuits. Moreover, these batteries do not need the extra safety layers cause the overall energy density to remain in high voltages and amperages [18–22]. In addition, based on especial phenomena in the solid electrolytes (such as that only Li^+ are mobile in solid electrolyte), several number of unfavorable parallel chemical reaction remove inside the electrolytes, which causes to increase the safety condition [23–26]. It is notable beside these advan-

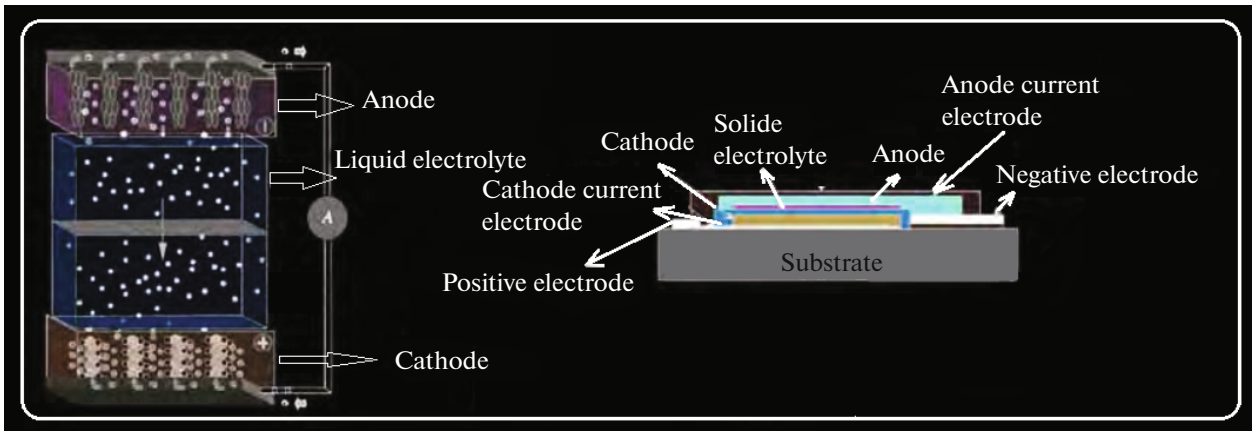

Fig. 1. A comparison of thin-film solid-state electrolyte with liquid electrolyte of a lithium-ion batteries battery.

tages there are some disadvantages as instance, solid state electrolytes (SSE) are not comparable with liquid electrolytes due to lower achievable conductivity. Our target of this study is a discussion of functional solid electrolytes LIBs for understanding the action of electrochemistry phenomenon. This work consists of developmental concept on solid electrolytes for manufacturing ways and characterization of these type electrodes. The initial step of this research was accomplished to synthesize and characterization a suitable conducting solid electrolytes. Interpreting the electrochemical properties for quick ion conduction via solid compounds is the key to fabrication of solid-electrolytes LIBs [27–32]. A proper understanding of chemical reactions inside the LIBs can be yielded through using cathode mixed materials as well as from selection proper composites for anodes during electrolyte/electrode interaction. Finally, our target was to exhibit the condition of a high energy density solid electrolyte rechargeable battery due to the efficiency of kinetic reactions of cathode and anode compounds resulting from decreasing of Nano particle sizes through electrochemical testing [33–37]. In this research, we assess solid-state interfaces with respect to a range of important factors: interphase formation, interface between cathode and inorganic electrolyte, interface between anode and inorganic electrolyte, interface between polymer electrolyte and Li metal, and interface of interparticles. This review also summarizes existing characterization strategies, including microscopy observation, chemical composition analysis, and electrochemical characterization.

2. ELECTROLYTE BACKGROUND OF LIBS

2.1. Organic Solid Polymers and Inorganic Solids

In total, solid electrolytes can be separated into two main categories: 1-organic solid polymers and 2-inorganic solids, containing oxides and sulfides, etc. [38]. Recently, several of solid electrolytes with superb ionic conductivity have shown great promise to replace current commercial organic electrolyte batteries, particularly for Li_{10}–GeP_2S_{12} and Li_2S–P_2S_5 with their high ionic conductivities of 1.3×10^{-2} S cm^{-1} and 1.8×10^{-2} S cm^{-1}, respectively. Their conductivities are comparable with that of organic liquid electrolyte (usually on the order of 10^{-2} S cm^{-1}, 25°C), confirming that solid electrolyte materials exhibit great promise for next-generation batteries [39, 40]. However, a key scientific issue that will hinder the practical application of SSBs concerns solid-solid interfaces.

2.2. Ionic Position in Cathode Materials

The lithium diffusion process appears with a current of Li^+ via the electrolyte, by a redox reaction and also through an external circuit. Insertion of Li^+ inside cathode materials is largely related to the interaction potential among all ions, particularly the Li^+ and the host compounds. These interactions are related to the properties of cathode compounds as follows:

$$W_t = W_C + W_P + W_r, \quad (1)$$

where W_t is the total potential energy, W_C is the Columbic interaction, W_P is the van der Waals interaction and W_r is the overlap repulsion among all shell ions. Obviously, "W_t" from insertion of Li^+ in a crystal should be calculated, and it is supposed that ion transport had been accomplished through an optimal potential. Based on the shape of the insertion in the crystal, several structure items can be presented and categorized as: 1-$LiFePO_4$, structures same as $LiCoO_2$, and 3-3D arrays of tunnels $LiMn_2O_4$. The cathode materials directly affect insertion amounts the Li-ion as it can be seen in Table 2. $LiCoO_2$, with two dimensional layered structures, exhibits the largest Li-ion diffusivity among the other classes, while $LiFePO_4$ with one-dimensional channels exhibits the lowest.

Recently, several quantum chemical calculations of Li_xCoO_2 diffusivity have been accomplished at varying amounts of Li ($0 \le x \le 1$), which indicate the reason of wide concentration of lithium insertion in electrolytes (Table 2). In addition, these calculations exhibited that (010) surface in $LiFePO_4$ has the optimum structure for Li^+ insertion according to the approximation of numerical data. Obviously, ab initio methods because of artificial modeling might be inapplicable for multiple phases, and disordered amorphous structure's calculations. The initial design for manipulating the diffusivity of Li^+ in cathode materials consists of doping, coating, and finally decreasing the cathode surface by Nano scaling of the particle size.

2.3. Interfaces in Solid State Batteries

We supposed the term "interface" as a combination of interphase formation, contact condition, energy status, and defects. Physical and chemical processes that take place at an interface during cycling should be taken into consideration. These essential processes include SEI formation, dendrite growth, Li-depleted space-charge layer, and interfacial adhesion variation due to structural and volume change, among others. The chemical stability of an electrolyte can be predicted using the energy diagram shown in Fig. 2. The "window" for both liquid and solid electrolytes can be determined by the energy separation E_g between the lowest unoccupied molecular orbital (LUMO) or conducting band (CB) and the highest occupied molecular orbital (HOMO) or valence band (VB) [63] of the electrolyte material, which is thermodynamically stable when the chemical potential (ma for anode and mc for cathode) of the electrode materials is within the LUMO–HOMO range. In other words, the interface is not stable if $m_a >$ LUMO (or CB) or $m_c <$ HOMO (or VB), unless an SEI forms at the interface as the passiv-

Table 2. Band Gap (eV) for cathode and anode electrodes

Electrodes/Condition	Cathode composite	Band Gap, eV	References
Anode and cathode materials	Copper(anode)	0	41, 42
	Graphite(anode)	0	43–44
	Aluminum(anode)	0	45
	$LiCoO_2$ (cathode)	0.6–2.5	46–48
	$LiMn_2O_4$(cathode)	0.25–2.1	49–51
	$LiFePO_4$(cathode)	0.2–0.9	52,53
Cathode materials	Li_xCoO_2	2.1×10^{-2}	54
	$Li_{1.0}Mg_yCo_{(1-y)}O_2$	$(10^{-3.7}y = 0)$; $(10^{-1.2}y = 0.04)$; $(10^{-0.70}y = 0.05)$	55
	$Li_xNi_{0.30}Co_{0.70}O_2$	10^{-4} to 10^{-3}: $0.70 < x < 1$	56
	$LiGa_yCo_{(1-y)}O_2$	6.65×10^{-4}: un-doped system	57
	$Li_xMn_2O_4$	$10^{-6.5}$ ($x = 1.00$)	49–51
	$Li_xMn_2O_4$	$10^{-4.5}$ ($x = 0.90$)	58
	$LiCo_yMn_{2-y}O_4$	$(2.3 \times 10^{-4}$ ($y = 0.1$); $(2.5 \times 10^{-2}$ ($y = 1$)	59
	$LiNi_yMn_{2-y}O_4$	0–4.5 ($y = 0$, to 0.6): at RT	60
	Li_xFePO_4	10^{-2}: $x = 0.8$ (impurity: $Fe_2P_2O_7$)	61
	$Li_{1-x}MxFePO_4$(M=Zr, Nb, Mg)	10^{-3} (size: 30 nm, C content: 5 wt %)	62

ation layer. The formation of SEI has been widely studied in liquid-electrolyte batteries, and the concept can potentially be extended to SSBs upon careful comparison of these two very different battery systems [64–66].

2.4. Electrical Position in Anode Materials

Interlayer interactions in graphite are too much low and due to the large distance between those layers, allowing Li-ions to easily move between these sheets. In addition, these intercalations cause unique crystal and electronic situations. In amorphous carbons, as the disorder appear, electrical conductivity considerably reduces. Since quantum calculation and ab-initio methods are not able to analyses the electronic situation of amorphous structure in graphite, several models have been developed to predict electrical conductivities in graphite [67, 68].

2.5. Measurement of Electrolytes Conduction

Since solvent electrolytes are extremely applied because of higher ionic conductivities, various electrolytes compounds have been analyzed as replacements, some of them do not exhibit an acceptable ionic conductivity at least for 10^{-3} S cm^{-1} conductivity in LIBs [69]. The importance of electrolytes is to create an ionic conduction among the electrolytes, anodic and cathodic electrodes. Therefore, the main concern in electrolyte investigation is for understandings how to increase ionic conductivity [70–72]. During dissolving cathode material salts in the $LiPF_6$ as an important electrolyte, the cathode ions (Li^+) and anions such as PF_6^- are produced. Since dissociation of the salt is relevant to the dialectical condition such as constant of the solvent, therefore with a high dielectric constant strong solvating occurs [73]. Consequently, large anions of any salts by high conductivity and solubility could be distributing their negative charges, properly.

2.6. SSE (Solid-State Electrolytes) Evaluation

SSE electrolytes have several advantages compared with liquid electrolytes such as a simple designing, a suitable sealing, resistance to any vibrations, resistance to pressure, explosion in high temperature, wide electro chemical stability and better safety [74–76]. The important disadvantage of these types of electrolytes is due to lower ionic to the conductivities. Ionic conductivities of several solid-state electrolytes are listed in Table 3 [77–87]. The ions movement of gelled macromolecules and polymers containing high solubility is considerably different from those crystalline materials [88, 89]. In the items of solvent free polymer electrolytes, the mobility of the host is a reason for the ionic motion; ions move only if the polymers undergo large-amplitude motions [90] related to the glass tran-

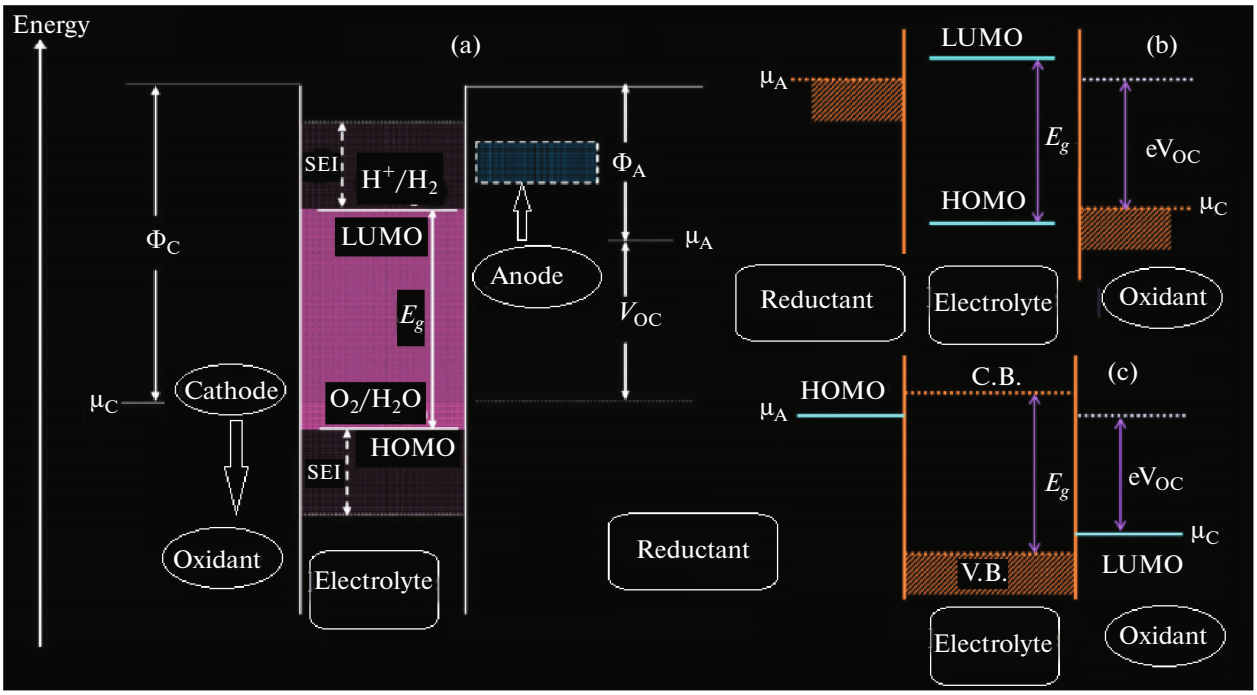

Fig. 2. A schematic representation of LUMO and HOMO liquid electrolyte, (a) Voc refers to the open-circuit voltage of the battery. (b) C.B. refers to the conducting band of solid electrolyte. (c) V.B. indicates the valance band.

sition temperature (T_g). Polymer electrolyte exhibits quick ionic situation above their T_g where they are bigger comprised of amorphous structures. Therefore, a low T_g polymer such as PEO (polyethylene oxide) [91] has become an important polymer host for solvent free electrolytes, and amorphous of this polymer is being researched [92, 93] as a model to increase its ionic conductivity. Gelled polymer exhibits quicker ionic conduction compared with free electrolytes, due to the diffusion of low molecular weight solvents in polymers [94, 95]. Solid electrolytes fabricated in semiconductors have also been used widely as an important ingredient of solid-state micro batteries. Moreover, inorganic elements applied for solid-state electrolytes often consist of rarer metals such as Ge, Ti, Sc, In, Lu, La and Y that are too much expensive [96]. Because of the mentioned problems for using the solid-state electrolytes, only gel polymer electrolytes have applied as commercial fabrication in markets [97].

One of the best electrolytes known to have all these criteria is an amorphous lithium phosphorus oxynitride, which was first synthesized by Bates in 1992. This compound, known as "LiPON" forms a uniform conformal coating free of grain boundaries and cracks. Electrical measurements by Yu have demonstrated LiPON films stable in contact with lithium metal, and cathode potentials up to 5.6 V [105] (Table 3). An ultra-thin LiPON also creates a significant efficiency in viewpoint of volume and mass for LIBs. Cells including LiPON have demonstrated perfect cycle life over 60000 cycles between 4.1 and 3.2 V without automatic discharge. Since the ionic conductivity of LiPON is too low, this electrolyte is usually useful only in a "thin film" configuration with solid electrolyte layer thicknesses around ~1000 nm. The thin film construction of batteries employing LiPON electrolyte limits overall capacity and therefore limits commercial application to small medical devices and MEMS devices. Fabricant of the LiSICON structure has been done to create a 3D rigid framework for moving alkali ions through internal spaces. LiSICON electrolytes are made based on the formula $Li_xM_2M'_3O_{12}$, where M and M' are generally metals and represent metal ions containing octahedral and tetrahedral coordinated to the O_2-ions such as $Li_8Mg_2Si_3O_{12}$ [106].

3. MATERIALS AND METHODS

3.1. High Conductivity Melt Quenching Method (Ball Milling)

All-solid-state batteries (ASSBs) have come into focus in recent years as energy storage devices with energy densities potentially exceeding those of conventional lithium-ion batteries (LIBs). However, in practice, severe problems still have to be solved. To reach high energy densities, it is indispensable to use lithium as anode and to build composite cathodes with high active material loading in the range of 85 wt %.

In past decades, several manufacturing techniques have been developed to prepare solid electrolytes, the

Table 3. Ionic conductivity of various non-solid and SSE

System	Solid state electrolytes (SSE)	Ionic conductivities, S cm^{-1}	References
In Salt	Wet polymer	8.5×10^{-7} (LiPF6 6 wt % in PVdF)	77
	Gel-polymer	7.8×10^{-2} (at 25°C)	78
	Plastic crystal	1×10^{-4} (6%), 5×10^{-3} (12%): $LiBF_4$	79
	Crystalline (perovskite)	1.0×10^{-3} ($x = 0$, 0.2)	80
	Crystalline (NASICON)	6.5×10^{-5} (at 200°C)	81
	Crystalline (thio-LISICON)	4.3×10^{-5} ($x = 0$)	82, 83
	Crystalline (Garnet)	5.2×10^{-4}	84
	Glass (LiPON)	1.8×10^{-6} to 7.7×10^{-7}	85
	Composite (glass + polymer)	1.2×10^{-3} (dry process)	86
	Glass-ceramics	1.3×10^{-8}	87
Solvent electrolytes			
Compounds	Solvent	conductivities, S cm^{-1}	References
$LiClO_4$	PC	5.5	98
$LiAsF_6$	EC/DMC	8.5	99, 100
$LiBF_4$	EC/DMC	11.3	101, 102
$LiPF_6$	EC/DMC	10.5	103, 104

most well-known being SSE, which is obtained by a high conductivity melt quenching method. During the preparation of SSE, an ionic conductivity of approximately 10^{-2} cm^{-1} was obtained and gave suitable electrochemical stability [107]. Although there are different methods for fusion systems, the cooling method is one of the most important cases in which it can be applied as an example of the usual method. In this way, the powders are first pressed through a suspension in a carbon-coated quartz tube and then vacuum sealed to obtain an ampoule of these materials. To prepare the glass substrate, the bulb is heated to 750°C for half a day to obtain a single phase and uniform shape. Later, the temperature of the quenched material must be reduced with cold water to produce a solid solution. For crystallization from solutes, the bulb should be heated to 750°C for half a day, and then the product can be kept for about two days at a certain temperature to promote nucleation and crystal growth [108]. Figure 3 shows a density of state diagram for different composites and phases such as 75% Li_2S with 25% P_2S_5 using for solid state electrolyte [84]. Recently, ball milling methods have been investigated the production of ultrafine amorphous products at 298 K. The ideal powders are suitable for achieving large ionic conductivities and are also used to achieve the best contact between electrolytes and electrodes in SSE [109, 110]. Ball milling probably also confirmed increased textural properties due to amorphous compounds, which are extracted using melt quenching techniques [111, 112]. Ball-milled amorphous powders (BMAPs) are sometimes heated strongly to obtain crystalline units capable of higher conductivity compared to previous powders [113, 114]. HEBM, which stands for High Energy Ball Milling, is an ideal technology for creating amorphous materials, and both contain the same concepts of pre-peel alloys using crushing technology. HEBM is generally carried out using shaker mills where the rotation takes place on a fixed axis.

Although high energy essentially causes a high attrition grinding motion, with consideration of certain elements and also proper control, the chambers rotating on a primary disk can be set at a selective speed. Since during grinding the compounds are alternately flattened, crushed and welded, the steel balls trap certain particles between their surfaces. These impacts with enormous energies can be severely destroyed the molecules and reshaped them atomically, eliminating unusual surfaces and other structural defects [114, 115]. Furthermore, deformation and cracking of composites results in a progressive decrease in particle size and leads to significantly lower diffusion distances and therefore temperatures [116–118]. BMAP is generally very stable and has stronger chemical interactions, which allows novel chemical reactions to be carried out while forming different nanostructures in our experiments [119].

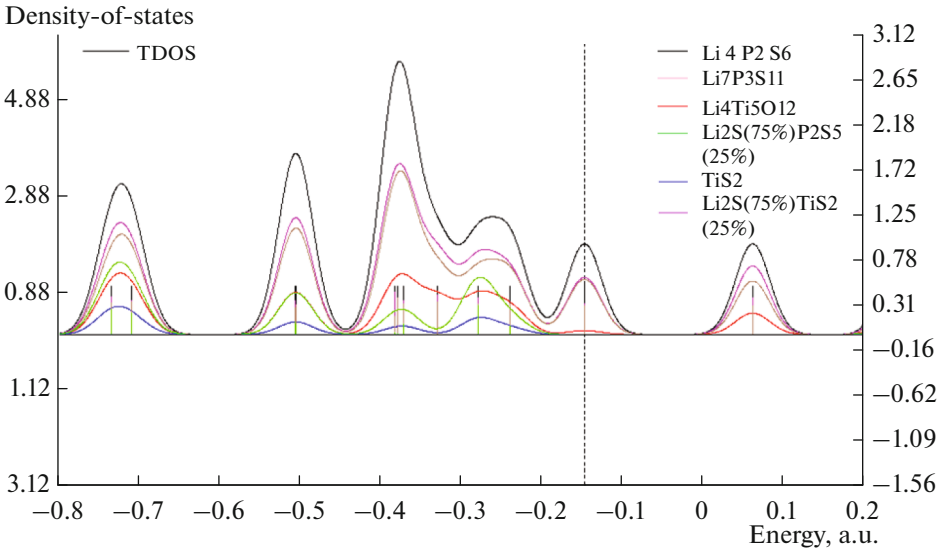

Fig. 3. Density of state diagram for different composites and phases such as 75% Li_2S with 25% P_2S_5 using for solid state electrolyte.

3.2. Single Step Ball Milling (SSBM)

Although ball milling followed by heat treatment has been shown to be effective, several steps of this process are time-consuming and inefficient, which should be modified. It is important to note that heat treatment typically produces glass-ceramic materials with larger particle size whose morphology may not be desirable for use in all-solid-state Li-ion batteries. A single-step ball milling (SSBM) procedure is proposed in this work in which ball milling and heat treatment are carried out simultaneously. By this work, we will report the glass-ceramic binary system $xLi_2S(100-x)P_2S_5$ produced by the SSBM process in terms of structural and electrochemical properties.

3.3. Experimental

3.3.1. Preparation of $Li_4P_2S_6$, $Li_4Ti_5O_{12}$, and combination of $P_2S_5/TiS_2/Li_2S$. The synthesis of $Li_4P_2S_6$ was done based on high temperature solid state reaction methods similar to procedures found in the literature Reagent-grade Li_2S (Aldrich, 99%) and P_2S_5 (Aldrich, 99%) crystalline powders were ground with a mortar and pestle for half hour and sealed in an evacuated quartz tube to form lithium thio-phosphate using the following reaction: $2Li_2S + P_2S_5 \rightarrow Li_4P_2S_6 + S$. For preparation of $Li_4Ti_5O_{12}$/carbon nanotubes composites were obtained by a solid-state sand milling method according to our published paper with some modifications. Firstly, stoichiometric amounts of Li_2CO_3, TiO_2, and carbon nanotubes solution (Jiang Su Cnano Technology Co. Ltd.) were dissolved in ethanol via sand-milling at 500 rpm for 0.5 h and subsequently at 2000 rpm for 3.5 h. Afterwards, the mixture was dried for 3 h into powder under 105°C. Then, the dried powders were calcined at 800°C for 5 h under Ar (Fig. 4). Necessary and sufficient for experiments have been considered as: Li_2S (Aldrich, 99%) and P_2S_5 (Aldrich, 99%) were applied as initial compounds for mechanical ball milling through using stoichiometry concentrations with proper fraction of zirconia exactly one gram with two zirconia balls (1 × 10 mm, 1 × 13 mm in diameter) for grinding. Energy ball milling took place for 24 h in a glove box containing Argon gas at a temperature controller around 60°C (Spex2000). Ball milled vials alternatively, were turned on and turned off to fix the temperature towards reaching the vial temperature. A perfect correlation was observed between the discrepancy ambient vial temperature and vials due to the milled without pausing. In addition to maintaining room temperature, vials were milled in 40-min intervals, frequently. All prepared materials from ball milled at room temperature were amorphous and interestingly, their conductivity amounts were confirmed with previously experiments values. In this work, we changed the amorphous materials into pellets 15 mm in diameter and 0.8 mm thick in a titanium die through cold press (5 metric tons). The products samples were characterized through X-ray diffraction using Cu Kα radiation and were sealed in an air isolated of aluminum box with beryllium vent and fixed on the X-ray diffract meter (PW3830). Diffraction amounts were evaluated for all morphological structures as well as unique materials between 15 and 45 deg. Ionic conductivities were calculated by AC impedance spectroscopy (Solartron 1280C) for all SSBM samples. Weighed composites then are cold pressed through 10 tons/metric pressures to prevent the lithium electrodes plates from being pressed to both sides of the pellet at one metric ton. The impedances of selected cells were calculated from 25 MHz to

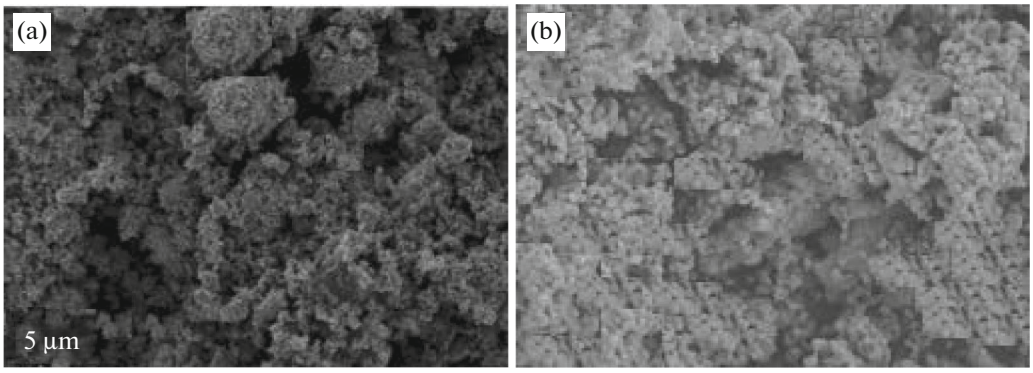

Fig. 4. Scanning electron microscopy (SEM) (a) $Li_4P_2S_6$, (b) $Li_4Ti_5O_{12}$ (10 μm) after ball milling.

110 mHz at 298 K and the conductivities were measured using complex impedance analysis. For providing TiS_2, several steps have been accomplished as follows 1—TiS_2 (Sigma-Aldrich, 99.0%) was ball milled in a 120 mL agate vial at a net weight of 600 mg. 2—large-ball-milled (LBM) samples were provided through 8 agate balls (8 mm diameter) and small-ball-milled (SBM) composites with 45 agate balls (5 mm diameter) for grinding. Ball milling took place for 3 h for large-ball-milled material and 6 h for small- ball-milled products in an Argon gas before the composites were used without further modification.

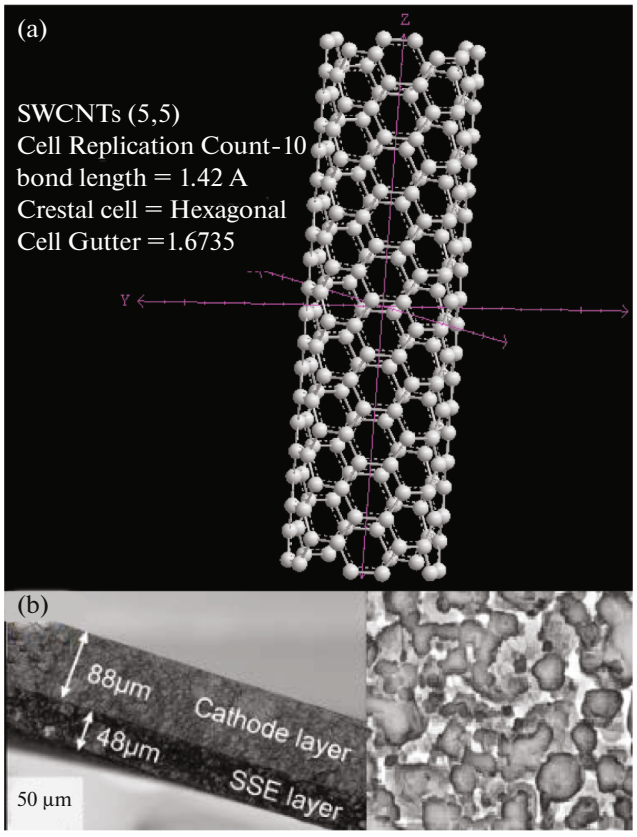

Fig. 5. Preparation materials including: (a) (5, 5) SWCNT and (b) SSE layers.

3.3.2. Preparation of anode materials. The capacity and performance of the battery not only depends largely on the intrinsic characteristics of the anode material but also on its morphology. Consequently, the suitable and appropriate structural design employed is much more important than the material selected. Many high-performance anode materials have been explored as novel materials for the next generation of LIBs. Anode electrode was made through a combination of crystalline Nano-silicon (n-Si) powder (50–100 nm, Sigma-Aldrich) and bulk silicon (B–Si) powder (1–45 μm, Alfa Aesar), solid-state electrolyte (SE) 76.0 Li_2S%–24.0P 2S 5% provided from ball milling methods and also multi-walled-carbon-nanotubes (NC7000) at a weight ratio of 1 : 6 : 1, respectively (Fig. 5a). We applied a conductive additive due to the increased contact surfaces (400 $m^2\ g^{-1}$) compared to acetylene black (65 $m^2\ g^{-1}$) and thus observed an acceptable increase in conductivity in our system. The double-layer pellets are produced by compressing one milligram of electrode material on top of 200 mg of SSE powder to five metric tons. Finally, the lithium sheet is pressed with SSE to the tune of one metric ton (Fig. 5b). All experiments and evaluations are performed in a poly-aryl-ether-ketone (PEEK) chip (I = 1.4 cm) and are also performed in an Ar-filled glove box with Ti metal rods as current collectors. Galvano/static measurement of charge-discharge cycling has been done for several items at a fixed density 110 mAg^{-1} at 298 K using an Arbin BT2000 galvanostat. The products samples were characterized through X-ray diffraction using Cu Kα radiation and were sealed in an air isolated aluminum box with beryllium vent and fixed on the X-ray diffract meter (PANalytical, PW3830).

3.3.3. Preparation of cathode materials. In SSE-LIBs using sulfide-based, high interfacial resistances among the cathode composite materials and the solid electrolyte have been seen during the initial charging process of $LiCoO_2$ as an effective cathode material. It

is obvious, which the high resistance is related to the destroying of the interface between the $LiCoO_2$ and the $Li_2S–P_2S_5$ solid electrolyte [120]. There are two ways of overcoming to this problem; 1-using electrolyte additives for enhancing ionic conductivities and fixing the electrolyte in contact with the electrode, and 2-Creating a favorable electrode/electrolyte interface by interfacial modification. It has been confirmed, which by using a network creating such as GeS_2 and SiS_2 to the $Li_2S–P_2S_5$ system, not only can be gained higher conductivities for SSE, better stability of the electrode/electrolyte system also can be formed [121]. By this second crystal structure such elements can be used that consist of large ionic radius and high polarizability, which consequently cause an increasing situation of mobility and conducting ions towards improving the solid crystal of the electrolytes [122].

These type additives materials have also exhibited to decrease the large chemical potential difference among the components of sulfide electrolyte as well as oxide electrode. Creating a suitable electrode/electrolyte system by optimization of cathode materials surfaces, has also confirmed an effective reduction of the resistance, through coatings of $Li_4Ti_5O_{12}$ on $LiCoO_2$ particles [123]. In addition, a novel molecule has been discovered as $Li_4Ti_5O_{12}$ to prevent dissolution [124], which the coating by this molecule prevent diffusion of the $LiCoO_2$ inside the electrolyte. In this study, we have investigated the mentioned additives in solid electrolytes to increase the stability of and contact electrode materials with electrolytes. $GeSe_2$ was used as a second network to improve the electrical conductivity and stabilize the SSE in our work, because sulfur is used as an additive to help stabilize the electrolyte for the high voltage in cathode electrodes. Finally, we applied Li_2O additive containing lithium increases the stability of the electrolyte/electrode interface by reducing the potential difference between the oxide cathode and the sulfide electrolyte.

$Li_2S–P_2S_5$ as SSE provided through ball milling as well as milling outputs in amorphous compounds elevated temperature conductivity of 8.99×10^{-3} S cm^{-1} and 9.93×10^{-4} S cm^{-1} respectively. Cathode composite materials were mixed by both balls milled and non-ball-milled of titanium sulfide powders and SSE at a ratio of 2 : 3 respectively. For composites containing acetylene black (Alfa-Aesar, 60% compressed) as a conductive additive, a ratio of 15 : 20 : 2 was applied for three compounds consist of TiS_2, solid electrolyte, and acetylene black, respectively. Battery pellets are made by cold-pressing (6 metric tons) 12 mg of the composite cathode electrode above 150 mg of SE for 5 min. Li foil (Alfa-Aesar, 0.70 mm thick) is then attached to the SSE surface at 3 metric tons. All pressing and testing products are accomplished in a polyaryletheretherketone (PEEK) mold (I = 1.5 cm) with Titanium rods as current collectors for both working and counter electrodes in an Ar-filled glove box (Fig. 6).

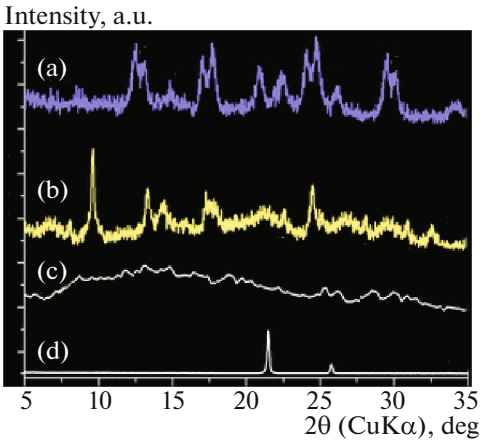

Fig. 6. XRD patterns of prepared samples. (a) Sample dried at 150°C, (b) Sample dried at 25°C, (c) P_2S_5, (d) Li_2S.

3.3.4. Electrolyte fabrication. $Li_2S–GeS_2–P_2S_5$ SSE was provided using the SSBM method [125–127]. Reagent-grade powders of Li_2S (Aldrich, 99.0%), P_2S_5 (Aldrich, 99%), and GeS_2 (City Chemical, 99.0%) were consumed as initial products. Suitable amounts of composites were mixed into a zirconia vial (Spex) at a net weight of 1.5 g with two zirconia balls for grinding. HEBM (Spex8000) tool was selected and kept for 15 h in an Ar-filled dry box. Heat action of SSBM: SSE powders were accomplished through initial mixing sulfur and SSE powders in pelletizing the powders at 6 metric tons in a stainless-steel die (I = 1.5 cm) with 500 mg of initial compounds. Provided pellets were fixed in a sealed glass container and heated to 250°C for 15 h. In the moment related to the point of the desired temperature, finished pellets were extracted from the hot plate and put them on a cooling rack. Then the heated pellets were ground in a mortar with pestle and used for solid battery production with no further modifications inside Argonne filled glove box.

$Li_2S–GeSe_2–P_2S_5$ ($Li_{4x}Ge_{1-x}P_xS_{2(1+x)}Se_{2(1-x)}$ electrolytes were prepared similarly with $GeSe_2$ (Stream, 99.9%) instead of GeS_2 was performed for 240, 350, and 450°C.

4. RESULTS AND DISCUSSION

4.1. Conductivities

LISICON phase of $Li_{(4-x)}Ge_{(1-x)}P_xS_4$ ($0.5 < x < 0.9$) by high conductivities created through monoclinic superstructure. We predicted that the amounts of enhancement conductivities provided mostly through SSBM around one or two orders of magnitude compared with other glass electrolytes as well as higher than those amounts for glass-ceramics, which were provided by two step heating. The SSBM glass-

ceramic sample with $x = 76$ was not as high as standard two step glass ceramics, but the SSBM glass-ceramic sample with $x = 80$ was comparably close in conductivity to the standard two step glass-ceramic sample. We attribute this discrepancy in conductivities for $x = 64$ to the lower temperature at which SSBM samples are exposed in comparison to standard heat treating. We speculate the entire SSBM conductivity curve can rise as a result of higher ball milling temperatures. More systematic studies on the effect of the ball milling temperature on ionic conductivity are in progress. The simplicity of the SSBM process and high ionic conductivity of SSBM samples make the SSBM method superior for development of SSE for all-solid-state battery production. Furthermore, the SSBM with no post heat treatment required, completely eliminates any potential grain growth of as-ball-milled fine powders.

4.1.1. MWCNTs as a conductive additive. It is usual to exhibit the specific capacities based on the mass of the active materials such as Nano-Si in the anode. In addition, the lithium interaction capacity of MWCNTs can considerably help to the total capacities of the anode materials. Consequently, the capacities of the conductive additives were gained in the cell using several amounts of the MWCNTs as the active material. The specific capacities of these amounts in the anode were then estimated from the data for the corresponding capacity of Nano-Si according to the use of MWCNTs amounts. We exhibited a considerable enhancing of the specific surface area of the MWCNTs ability to flex in order to maintain electrical contact with the Nano-Si particles upon cycling. This test confirms that solid state lithium batteries using Nano-Si and MWCNTs as a conductive additive maintain a capacity considerably and amazingly exhibit higher efficiency compared with those batteries without using Nano-Si. MWCNTs were exhibited to improve cycling capacity in all-solid-state lithium batteries over acetylene black as a conductive additive.

CONCLUSIONS

A proper understanding of chemical reactions inside the LIBs can be yielded through using cathode mixed materials as well as from selection proper composites for anodes during electrolyte/electrode interaction. Finally, our target is based on the condition of a high energy density solid electrolyte rechargeable battery due to the efficiency of kinetic reactions of cathode and anode compounds resulting from decreasing of Nano particle sizes through electrochemical testing. Therefore, due to a suitable fabricate LIBs with extreme degree of safety; the liquid electrolytes should be changed with solid electrolytes. Solid electrolyte has several advantages compared with liquid electrolytes including large stability, long life containing durable properties, non-flammable, and insulate for preventing thermal increasing inside internal circuits.

FUNDING

This work was supported by ongoing institutional funding. No additional grants to carry out or direct this particular research were obtained.

CONFLICT OF INTEREST

The authors of this work declare that they have no conflicts of interest.

REFERENCES

1. J. B. Goodenough and K.-S. Park, "The Li-ion rechargeable battery: A perspective," J. Am. Chem. Soc. **135**, 1167–1176 (2013). https://doi.org/10.1021/ja3091438
2. I. Y. Gudkova, I. N. Zyuzin, and D. B. Lempert, Russ. J. Phys. Chem. B **16**, 58–65 (2022). https://doi.org/10.1134/S1990793122010067
3. V. F. Gromov, M. I. Ikim, G. N. Gerasimov, et al., Russ. J. Phys. Chem. B **16**, 138–140 (2022). https://doi.org/10.1134/S1990793122010055
4. E. A. Lebedeva, S. A. Astaf'eva, and T. S. Istomina, Russ. J. Phys. Chem. B **16**, 316–322 (2022). https://doi.org/10.1134/S1990793122010109
5. A. M. Kuperman, A. Y. Sergeev, R. A. Turusov, et al., Russ. J. Phys. Chem. B **16**, 1172–1179 (2022). https://doi.org/10.1134/S1990793122060070
6. Kh. S. Daliev, Sh. B. Utamuradova, J. J. Khamdamov, et al., Adv. Phys. Res. **6**, 42–49 (2024). https://doi.org/10.62476/apr61.49
7. A. T. Mamadalimov, M. Sh. Isaev, M. K. Karimov, et al., Adv. Phys. Res. **6**, 50–55 (2024). https://doi.org/10.62476/apr61.55
8. F. Mollaamin and M. Monajjemi, Russ. J. Phys. Chem. B **18**, 1199–1216 (2024). https://doi.org/10.1134/S1990793124700519
9. F. Mollaamin and M. Monajjemi, Russ. J. Phys. Chem. B **18**, 533–548 (2024). https://doi.org/10.1134/S199079312402012X
10. F. Mollaamin and M. Monajjemi, Russ. J. Phys. Chem. B **18**, 49–66 (2024). https://doi.org/10.1134/S1990793124010159
11. F. Mollaamin, S. Mohammadi, Z. Khalaj, et al., Russ. J. Phys. Chem. B **18**, 67–82 (2024). https://doi.org/10.1134/S1990793124010330
12. B. Li, S. Li, J. Xu, et al., Energy Environ. Sci. **9**, 2025–2030 (2016). https://doi.org/10.1039/C6EE01019A
13. S.-H. Chung, C.-H. Chang, and A. Manthiram, Energy Environ. Sci. **9**, 3188–3200 (2016). https://doi.org/10.1039/C6EE01280A
14. J. Liu, D. G. D. Galpaya, L. Yan, et al., Energy Environ. Sci. **10**, 750–755 (2017). https://doi.org/10.1039/C6EE03033E

15. U. V. Alpen, A. Rabenau, and G. H. Talat, Appl. Phys. Lett. **30**, 621–623 (1977). https://doi.org/10.1063/1.89283
16. K. Kanehori, K. Matsumoto, K. Miyauchi, et al., Solid State Ionics **9–10**, 1445–1448 (1983). https://doi.org/10.1016/0167-2738(83)90192-3
17. J. Fu, Solid State Ionics **96**, 195–200 (1997). https://doi.org/10.1016/S0167-2738(97)00018-0
18. L. K. Abdullayeva and M. H. Hasanov, New Mater. Compd. Appl. **8**, 135–141 (2024). https://doi.org/10.62476/nmca8135
19. F. Mollaamin, S. Shahriari, and M. Monajjemi, Russ. J. Phys. Chem. B **18**, 398–418 (2024). https://doi.org/10.1134/S199079312402026X
20. R. R. Kayumov, A. P. Radaeva, and A. A. Krupina, Russ. J. Phys. Chem. B **17**, 801–809 (2023). https://doi.org/10.1134/S1990793123040097
21. Kh. Kh. Hashimov and T. M. Isayeva, New Mater. Compd. Appl. **8**, 121–134 (2024). https://doi.org/10.62476/nmca8121
22. M. Monajjemi, F. Mollaamin, S. Shahriari, et al., Russ. J. Phys. Chem. B **18**, 1090–1112 (2024). https://doi.org/10.1134/S1990793124700465
23. F. Mollaamin, Russ. J. Phys. Chem. B **18**, 805–820 (2024). https://doi.org/10.1134/S1990793124700131
24. L. K. Abdullayeva and M. H. Hasanov, New Mater. Compd. Appl. **8**, 135–141(2024). https://doi.org/10.62476/nmca8135
25. F. Mollaamin and M. Monajjemi, Russ. J. Phys. Chem. B **18**, 607–623 (2024). https://doi.org/10.1134/S1990793124020271
26. F. Mollaamin, A. Ilkhani, N. Sakhaei, et al., J. Comput. Theor. Nanosci. **12**, 3148–3154 (2015). https://doi.org/10.1166/jctn.2015.4092
27. M. Monajjemi, L. Mahdavian, F. Mollaamin, et al., Russ. J. Inorg. Chem. **54**, 1465–1473 (2009). https://doi.org/10.1134/S0036023609090216
28. F. Mollaamin and M. Monajjemi, Russ. J. Phys. Chem. B **17**, 658–672 (2023). https://doi.org/10.1134/S1990793123030223
29. M. Monajjemi, A. Sobhanmanesh and F. Mollaamin, Fulleren Nanotubes Carbon Nanostruct. **21**, 47–63 (2013). https://doi.org/10.1080/1536383X.2011.574325
30. M. Monajjemi, M. H. Razavian, F. Mollaamin, et al., Russ. J. Phys. Chem. A **82**, 2277–2285 (2008). https://doi.org/10.1134/S0036024408130207
31. M. Monajjemi, N. Karachi, and F. Mollaamin, Fulleren Nanotubes Carbon Nanostruct. **22**, 643–662 (2014). https://doi.org/10.1080/1536383X.2012.717557
32. A. F. Gochuyeva, A. M. Mehdiyeva, and S. V. Bakhshaliyeva, New Mater. Compd. Appl. **8**, 87–93 (2024). https://doi.org/10.62476/nmca8187
33. M. Monajjemi, F. Mollaamin, S. Shahriari, et al., Russ. J. Phys. Chem. B **18**, 1217–1225 (2024). https://doi.org/10.1134/S1990793124700349
34. A. A. Abdullayeva, N. E. Ahmedova, G. T. Atakishiyeva, et al., New Mater. Compd. Appl. **8**, 149–161 (2024). https://doi.org/10.62476/nmca82149
35. F. Mollaamin and M. Monajjemi, Russ. J. Phys. Chem. B **18**, 1177–1198 (2024). https://doi.org/10.1134/S1990793124700507
36. M. Al-Shuwaili, H. Mahdi, and M. Makram, New Mater. Compd. Appl. **8**, 289–301 (2024). https://doi.org/10.62476/nmca82289
37. F. Mollaamin and M. Monajjemi, Russ. J. Phys. Chem. B **18**, 1199–1216 (2024). https://doi.org/10.1134/S1990793124700519
38. B. Khalili Hadad, F. Mollaamin, and M. Monajjemi, Russ. Chem. Bull. **60**, 238–241 (2011). https://doi.org/10.1007/s11172-011-0039-5
39. N. Kamaya, K. Homma, Y. Yamakawa, et al., Nat. Mater. **10**, 682–686 (2011). https://doi.org/10.1038/nmat3066
40. Y. Seino, T. Ota, K. Takada, et al., Energy Environ. Sci. **7**, 627–631 (2014). https://doi.org/10.1039/C3EE41655K
41. W. D. Callister Jr., *Materials Science and Engineering: An Introduction*, 4th ed. (John Wiley and Sons, 1997), pp. 796–801.
42. K. S. Novoselov, A. K. Geim, S. V. Morozov, et al., Science **306**, 666–669 (2004). https://doi.org/10.1126/science.110289
43. B. Partoens and F. M. Peeters, Phys. Rev. B **74**, 075404 (2006). https://doi.org/10.1103/PhysRevB.74.075404
44. M. Hess, E. Lebraud, and A. Levasseur, J. Power Sources 68, 204–207 (1997). https://doi.org/10.1016/S0378-7753(96)02553-0
45. B. Segall, Phys. Rev. **124**, 1797–1806 (1961). https://doi.org/10.1103/PhysRev.124.1797
46. J. P. Kemp and P. A. Cox, J. Phys. Condens. Matter **2**, 9653–9667 (1990). https://doi.org/10.1088/0953-8984/2/48/018
47. S. Shi, C. Ouyang, M. Lei, et al., J. Power Sources **171**, 908–912 (2007). https://doi.org/10.1016/j.jpowsour.2007.07.005
48. J. van Elp, J. L. Wieland, H. Eskes, et al., Phys. Rev. B **44**, 6090–6103 (1991). https://doi.org/10.1103/PhysRevB.44.6090
49. K. Ragavendran, A. Nakkiran, P. Kalyani, et al., Chem. Phys. Lett. **456**, 110–115 (2008). https://doi.org/10.1016/j.cplett.2008.03.016
50. J. Marzec, K. Swierczek, J. Przewoznik, et al., Solid State Ionics **146**, 225–237 (2002).
51. J. Molenda and W. Kucza, Solid State Ionics **117**, 41–46 (1999). https://doi.org/10.1016/S0167-2738(99)00121-6
52. S. Shi, L. Liu, C. Ouyang, et al., Phys. Rev. B **68**, 195108 (2003). https://doi.org/10.1103/PhysRevB.68.195108
53. Y. N. Xu, S. Y. Chung, J. T. Bloking, et al., Electrochem. Solid-State Lett. **7**, A131–A134 (2004). https://doi.org/10.1149/1.1703470
54. Y. Takahashi, N. Kijima, K. Tokiwa, et al., J. Phys. Condens. Matter **19**, 436202 (2007). https://doi.org/10.1088/0953-8984/19/43/436202

55. S. Levasseur, M. Ménétrier, C. Delmas, Chem. Mater. **14**, 3584–3590 (2002). https://doi.org/10.1021/cm021107j
56. Y. Takahashi, N. Kijima, K. Tokiwa, et al., J. Phys. Condens. Matter **19**, 436202 (2007). https://doi.org/10.1088/0953-8984/19/43/436202
57. S. M. Lala, L. A. Montoro, V. Lemos, et al., Electrochim. Acta **51**, 7–13 (2005). https://doi.org/10.1016/j.electacta.2005.04.001
58. J. Molenda, W. Ojczyk, M. Marzec, et al., Solid Sate Ionics **157**, 73–79 (2003). https://doi.org/10.1016/S0167-2738(02)00191-1
59. J. Molenda, K. Swierczek, J. Marzec, et al., Solid State Ionics **157**, 101–108 (2003). https://doi.org/10.1016/S0167-2738(02)00195-9
60. M. G. Lazarraga, L. Pascual, H. Gadjov, et al., J. Mater. Chem. **14**, 1640–1647 (2004). https://doi.org/10.1039/B314157H
61. D. K. Kim, H. M. Park, S. J. Jung, et al., J. Power Sources **159**, 237–240 (2006). https://doi.org/10.1016/j.jpowsour.2006.04.086
62. F. Zhou, M. Cococcioni, C. A. Marianetti, D. Morgan, and G. Ceder, Phys. Rev. B **70**, 235121 (2004). https://doi.org/10.1103/PhysRevB.70.235121
63. J. B. Goodenough and Y. Kim, Chem. Mater. **22**, 587–603 (2010). https://doi.org/10.1021/cm901452z
64. M. Monajjemi, H. Yamola, and F. Mollaamin, Fulleren Nanotubes Carbon Nanostruct. **22**, 595–603 (2014). https://doi.org/10.1080/1536383X.2012.702163
65. F. Mollaamin, F. Najafi, M. Khaleghian, et al., Fulleren Nanotubes Carbon Nanostruct. **19**, 653–667 (2011). https://doi.org/10.1080/1536383X.2010.504956
66. M. Monajjemi, M. Khaleghian, N. Tadayonpour, et al., Int. J. Nanosci. **09**, 517–529 (2010). https://doi.org/10.1142/S0219581X10007071
67. L. Ravagnan, P. Piseri, M. Bruzzi, et al., Phys. Rev. Lett. **98**, 216103 (2007). https://doi.org/10.1103/PhysRevLett.98.216103
68. P. N. Vishwakarma and S. V. Subramanyam, J. Appl. Phys. **100**, 113702 (2006). https://doi.org/10.1063/1.2372585
69. R. J. Brodd, W. Huang, J. R. Akridge, Macromolecular Symposia **159**, 229–245 (2000). https://doi.org/10.1002/1521-3900(200010)159:1<229::AID-MASY229>3.0.CO;2-O
70. F. Mollaamin, M. Monajjemi, S. Salemi, et al., Fulleren Nanotubes Carbon Nanostruct. 19, 182 (2011). https://doi.org/10.1080/15363831003782932
71. F. Mollaamin and M. Monajjemi, J. Cluster Sci. **34**, 2901–2918 (2023). https://doi.org/10.1007/s10876-023-02436-5
72. F. Mollaamin and M. Monajjemi, J. Mol. Model. **29**, 119 (2023). https://doi.org/10.1007/s00894-023-05526-3
73. W. Zheng, Z. Li, K. Chen, et al., Molecules **27**, 6337 (2022). https://doi.org/10.3390/molecules27196337
74. F. Mollaamin and M. Monajjemi, Mol. Simulat. **49**, 365–376 (2023). https://doi.org/10.1080/08927022.2022.2159996
75. F. Mollaamin, S. Shahriari, M. Monajjemi, et al., J. Cluster Sci. **34**, 1547–1562 (2023). https://doi.org/10.1007/s10876-022-02335-1
76. F. Mollaamin and M. Monajjemi, J. Mol. Model. **29**, 170 (2023). https://doi.org/10.1007/s00894-023-05567-8
77. C. Y. Chiang, Y. J. Shen, M. Jaipal Reddy, and Peter P. Chu, J. Power Sources **123**, 222–229 (2003). https://doi.org/10.1016/S0378-7753(03)00514-7
78. M. Kaneko, M. Nakayama, and M. Wakihara, J. Solid State Electrochem. **11**, 1071–1076 (2007). https://doi.org/10.1007/s10008-006-0239-3
79. M. Egashira, H. Todo, N. Yosimoto, et al., J. Power Sources **178**, 729–735 (2008). https://doi.org/10.1016/j.jpowsour.2007.10.063
80. S. Zhang, J. Y. Lee, and L. Hong, J. Power Sources **134**, 95–102 (2004). https://doi.org/10.1016/j.jpowsour.2004.02.017
81. A. Abouimrane, P. S. Whitfield, S. Niketic, et al., J. Power Sources **174**, 883–888 (2007). https://doi.org/10.1016/j.jpowsour.2007.06.103
82. K. Y. Yang, K. Z. Fung, I. C. Leu, J. Alloys Compd. **438**, 207–216 (2007). https://doi.org/10.1016/j.jallcom.2006.07.116
83. T. Savitha, S. Selvasekarapandian, C. S. Ramya, et al., J. Power Sources **157**, 533–536 (2006). https://doi.org/10.1016/j.jpowsour.2005.07.071
84. R. Kanno, T. Hata, Y. Kawamoto, et al., Solid State Ionics **130**, 97–104 (2000). https://doi.org/10.1016/S0167-2738(00)00277-0
85. Y. Tomita, H. Matsushita, K. Kobayashi, et al., Solid State Ionics **179**, 867–870 (2008). https://doi.org/10.1016/j.ssi.2008.02.012
86. V. Thangadurai, J. Schwenzel, and W. Weppner, Ionics **11**, 11–23 (2005). https://doi.org/10.1007/BF02430397
87. Y. Hamon, A. Douard, F. Sabary, et al., Solid State Ionics **177**, 257–261 (2006). https://doi.org/10.1016/j.ssi.2005.10.021
88. J. H. Kennedy and Z. Zhang, J. Electrochem. Soc. **135**, 859–862 (1988). https://doi.org/10.1149/1.2095811
89. T. Inada, K. Takada, A. Kajiyama, et al., Solid State Ionics **158**, 275–280 (2003). https://doi.org/10.1016/S0167-2738(02)00889-5
90. B. V. R. Chowdari, G. V. Subba Rao, G. Y. H. Lee, Solid State Ionics **136–137**, 1067–1075 (2000). https://doi.org/10.1016/S0167-2738(00)00500-2
91. Y. Seino, K. Takada, B. C. Kim, et al., Solid State Ionics **176**, 2389–2393 (2005). https://doi.org/10.1016/j.ssi.2005.03.026
92. M. A. Ratner and D. F. Shriver, Chem. Rev. **88**, 109–124 (1988). https://doi.org/10.1021/cr00083a006
93. B. L. Papke, M. A. Ratner, and D. F. Shriver, J. Electrochem. Soc. **129**, 1694–1701 (1982). https://doi.org/10.1149/1.2124252

94. *Polymer Handbook*, Ed. by J. Brandup, E. H. Immergut, and E. A. Grulke, 4th ed. (John Wiley and Sons, 1999).

95. J. F. Le Nest, S. Callens, A. Gandini, et al., Electrochim. Acta **37**, 1585–1588 (1992). https://doi.org/10.1016/0013-4686(92)80116-4

96. A. Nishimoto, M. Watanabe, Y. Ikeda, et al., Electrochim. Acta **43**, 1177–1184 (1998). https://doi.org/10.1016/S0013-4686(97)10017-2

97. K. Aruchamy, S. Ramasundaram, S. Divya, et al., Gels **9**, 585 (2023). https://doi.org/10.3390/gels9070585

98. C. Svanberg, J. Adebahr, R. Bergman, et al., Solid State Ionics **136–137**, 1147–1152 (2000). https://doi.org/10.1016/S0167-2738(00)00610-X

99. M. J. G. Jak, F. G. B. Ooms, E. M. Kelder, et al., J. Power Sources **80**, 83–89 (1999). https://doi.org/10.1016/S0378-7753(99)00064-6

100. J.-M. Tarascon, A. S. Gozdz, C. Schmutz, et al., Solid State Ionics **86–88**, 49–54 (1996). https://doi.org/10.1016/0167-2738(96)00330-X

101. K. Xu, Chem. Rev. **104**, 4303–4418 (2004). https://doi.org/10.1021/cr030203g

102. M. Ue and S. Mori, J. Electrochem. Soc. **142**, 2577–2581 (1995). https://doi.org/10.1149/1.2050056

103. M. Schmidta, U. Heidera, A. Kuehnera, et al., J. Power Sources **97–98**, 557–560 (2001). https://doi.org/10.1016/S0378-7753(01)00640-1

104. C. W. Walker Jr., J. D. Cox, and M. Salomon, J. Electrochem. Soc. **143**, L80–L82 (1996). https://doi.org/10.1149/1.1836607

105. J. Bates, N. Dudney, B. Neudecker, et al., Solid State Ionics **135**, 33–45 (2000). https://doi.org/10.1016/S0167-2738(00)00327-1

106. H. Hong, Mater. Res. Bull. **13,** 117–124 (1978). https://doi.org/10.1016/0025-5408(78)90075-2

107. M. Monajjemi, F. Mollaamin, M. R. Gholami, et al., Main Group Metal Chem. **26**, 349–361 (2003). https://doi.org/10.1515/MGMC.2003.26.6.349

108. A. Hayashi, S. Hama, F. Mizuno, et al., Solid State Ionics **175**, 683–686 (2004). https://doi.org/10.1016/j.ssi.2004.08.036

109. A. Hayashi, S. Hama, T. Minami, et al., Electrochem. Commun. **5**, 111–114 (2003). https://doi.org/10.1016/S1388-2481(02)00555-6

110. N. Machida, H. Yamamoto, S. Asano, et al., Solid State Ionics **176**, 473–479 (2005). https://doi.org/10.1016/j.ssi.2004.08.019

111. H. Yamamoto, N. Machida, and T. Shigematsu, Solid State Ionics **175**, 707–711 (2004). https://doi.org/10.1016/j.ssi.2004.08.028

112. M. Tatsumisago, Solid State Ionics **175**, 13–18 (2004). https://doi.org/10.1016/j.ssi.2004.09.012

113. M. Tatsumisago, F. Mizuno, and A. Hayashi, J. Power Sources **159**, 193–199 (2006). https://doi.org/10.1016/j.jpowsour.2006.04.037

114. C. C. Koch, "Amorphization by mechanical alloying," J. Non-Cryst. Solids **117** (1990) 670–678. https://doi.org/10.1016/0022-3093(90)90620-2

115. E. Zhou, C. Suryanarayana, and F. H. (Sam) Froes, Mater. Lett. **23**, 27–31 (1995). https://doi.org/10.1016/0167-577X(95)00009-7

116. G. Le Caër and P. Matteazzi, Hyperfine Interact. **90**, 229–242 (1994). https://doi.org/10.1007/BF02069130

117. G. B. Schaffer and P. G. McCormick, Appl. Phys. Lett. **55**, 45–46 (1989). https://doi.org/10.1063/1.101750

118. J. Yu, Y. Chen, R. Wuhrer, et al., Chem. Mater. **17**, 5172–5176 (2005). https://doi.org/10.1021/cm050966f

119. Y. Chen, C. P. Li, H. Chen, et al., Sci. Technol. Adv. Mater **7**, 839–846 (2006). https://doi.org/10.1016/j.stam.2006.11.014

120. J. Wang, J. Yang, C. Wan, et al., Adv. Funct. Mater. **13**, 487–492 (2003). https://doi.org/10.1002/adfm.200304284

121. M. Armand and J.-M. Tarascon, Nature **451**, 652–657 (2008). https://doi.org/10.1038/451652a

122. Y.-G. Guo, J.-S. Hu, and L.-J. Wan, Adv. Mater. **20**, 2878–2887 (2008). https://doi.org/10.1002/adma.200800627

123. A. Sakuda, A. Hayashi, and T. Ohtomo, J. Power Sources **196**, 6735–6741 (2011). https://doi.org/10.1016/j.jpowsour.2010.10.103

124. J. E.Trevey, Y. S. Jung, and S. H. Lee, J. Power Sources **195**, 4984–4989 (2010). https://doi.org/10.1016/j.jpowsour.2010.02.042

125. F. Mollaamin and M. Monajjemi, J. Mol. Struct. **1300**, 137214 (2024). https://doi.org/10.1016/j.molstruc.2023.137214

126. F. Mollaamin and M. Monajjemi, Int. J. Quantum Chem. **124**, e27348 (2024). https://doi.org/10.1002/qua.27348

127. M. A. A. Zadeh, H. Lari, L. Kharghanian, et al., J. Comput. Theor. Nanosci. **12**, 4358 (2015). https://doi.org/10.1166/jctn.2015.4366